Influence of Nanoparticles Phenomena on the Peristaltic Flow of Pseudoplastic Fluid in an Inclined Asymmetric Channel with Different Wave Forms

Akram, Safia*[+]

Department of Basic Sciences, MCS, National University of Sciences and Technology, Islamabad 44000, PAKISTAN

Nadeem, Sohail

Department of Mathematics, Quaid-i-Azam University 45320, Islamabad 44000, PAKISTAN

ABSTRACT: *The influence of nanofluid with different wave forms in the presence of inclined asymmetric channel on peristaltic transport of a pseudoplastic fluid is examined. The governing equations for two dimensional and two directional flows of a pseudoplastic fluid along with nanofluid are modeled and then simplified under the assumptions of long wavelength and low Reynolds number approximation. The exact solutions for temperature and nano particle volume fraction are calculated. Series solution of the stream function and pressure gradient are carried out using perturbation technique. The flow quantities have been examined for various physical parameters of interest. It was found that the magnitude value of the velocity profile decreases with an increase in Q and ζ and increases in sinusoidal, multisinsoidal, trapezoidal and triangular waves. It was also observed that the size of the trapping bolus decreases with the decrease in the width of the channel d and increases with an increase in ξ.*

KEYWORDS: *Nano fluid particles; Peristaltic flow; Pseudoplastic fluid; Different wave forms; Inclined asymmetric channel.*

INTRODUCTION

The study of nanofluids has achieved considerable importance among the researchers because of its applications in sciences and industry. Nanofluids are the embryonic mixtures consist of solid particles disseminated in the conventional heat transfer base fluids. Base fluids (like water, ethylene glycol etc.) have ability to increase the effective thermal conductivity of nanofluids. The theory of nano fluids was first given by *Choi* [1]. *Selvakumar & Suresh* [2] have examined the convective performance of CuO/water nanofluid in an electronic heat sink.

** To whom correspondence should be addressed.*
+ E-mail: drsafiaakram@gmail.com ; safia_akram@yahoomail.com
1021-9986/2017/2/107-124 18/$/6.80

In their analysis they pointed out that nanoparticles dispersed in the base fluids have overcome the limitations of micron sized particles. *Bachok et al.* [3] have examined the unsteady boundary layer flow and heat transfer of a two dimensional nanofluid over a permeable stretching or shrinking sheet. Natural convective boundary layer flow of a nanofluid past a convectively heated vertical plate has been examined by *Aziz & Khan* [4]. In another study, *Aziz et al.* [5] have presented the free convection boundary layer flow past a horizontal flat plate embedded in porous medium filled by nanofluid containing gyrotactic microorganisms. Some recent studies of nano fluid on different flow problems are given in Refs. [6-12].

Peristalsis is a mechanism which is produced by successive waves of contraction which pushes their fluid (or fluid like contents) forward. Since the first investigation done by *Latham* [13], many researchers have discussed the peristaltic flows of Newtonian and non-Newtonian fluids with different flow geometries. *Eytan & Elad* [14] have highlighted the importance of peristaltic flows in asymmetric channel. *Tripath* [15] has examined the peristaltic transport of a viscoelastic fluid in a channel. Nonlinear peristaltic transport of a Newtonian fluid in an inclined asymmetric channel through a porous medium has been investigated by *Kothandapani and Srinivas* [16]. *Srinivas et al.* [17] have examined the mixed convection heat and mass transfer in an asymmetric channel with peristalsis. Effects of partial slip on the peristaltic flow of a MHD Newtonian fluid in an asymmetric channel have been done by *Yilidirim & Sezer* [18]. *Nadeem & Akbar* [19] have highlighted the study of influence of heat and mass transfer on the peristaltic transport of a Jeffrey-six constant fluid in an annulus. Nonlinear peristaltic flow of a fourth grade fluid in an inclined asymmetric channel have been discussed by *Haroun* [20]. In another paper *Haroun* [21] has examined the effect of Deborah number and phase difference on peristaltic transport of third order fluid in an asymmetric channel. For some relevant work of interest, the reader is referred to [22-24].

Motivated from the above analysis, the aim of the present paper is to examine the effects of nano-particles on the peristaltic flow of a Pseudoplastic fluid in an inclined asymmetric channel. The governing equations of Pseudoplastic fluid for two dimensional flow in Cartesian coordinate system are modelled along with heat transfer analysis and nanoparticle volume fraction. The highly nonlinear equations are simplified using some assumptions (like long wave length and low Reynolds number). The reduced equations are solved analytically with the help of regular perturbation technique. The physical features of the pertinent parameters are discussed by plotting the graphs of velocity, pressure rise, pressure gradient and stream lines.

THEORITICAL SECTION

Mathematical formulation

Let us consider the peristaltic transport of an incompressible nano non-Newtonian fluid (pseudoplastic fluid) in a two dimensional channel of width d_1+d_2. The channel is inclined at angle β. The channel asymmetry is produced due to different amplitudes and phases of the peristaltic waves. Heat transfer along with nano particle phenomena has been taken into description. The lower wall of the channel is sustained at temperature T_1 and nano particle volume fraction C_1 while the upper wall has temperature T_0 and nano particle volume fraction C_0.

The geometry of the wall surface is defined as

$$Y = H_1 = d_1 + a_1 \cos\left[\frac{2\pi}{\lambda}(X - ct)\right], \tag{1}$$

$$Y = H_2 = -d_2 - b_1 \cos\left[\frac{2\pi}{\lambda}(X - ct) + \varphi\right],$$

Where a_1 and b_1 are the amplitudes of the waves, λ is the wave length, d_1+d_2 is the width of the channel, c is the velocity of propagation, t is the time and X is the direction of wave propagation, the phase difference ϕ varies in the range $0 \le \phi \le \pi$, $\phi = 0$ corresponds to symmetric channel with waves out of phase and $\phi = \pi$ the waves are in phase, and further a_1, b_1, d_1, d_2 and ϕ satisfies the condition

$$a_1^2 + b_1^2 + 2a_1 b_1 \cos\varphi \le (d_1 + d_2)^2.$$

The equations governing the flow are given by the continuity equation

$$\nabla \cdot \mathbf{V} = 0, \tag{2}$$

The equation of motion

$$\rho_f \left(\frac{\partial \mathbf{V}}{\partial t} + (\mathbf{V} \cdot \nabla)\mathbf{V}\right) = \mathrm{div}\,\boldsymbol{\tau} + \mathbf{f}, \tag{3}$$

where

$$\boldsymbol{\tau} = -P\mathbf{I} + \mathbf{S}$$

in which the extra stress tensor **S** for pseudoplastic fluid is defined as [25]

$$\mathbf{S}, + \lambda_1 \mathbf{S}^{\nabla} + \frac{1}{2}(\lambda_1 - \mu_1)\left(\mathbf{A}_1\mathbf{S} + \mathbf{S}\mathbf{A}_1\right) = \mu\mathbf{A}_1, \quad (4)$$

$$\mathbf{S}^{\nabla} = \frac{d\mathbf{S}}{dt} - \mathbf{S}\mathbf{L}^{T} - \mathbf{L}\mathbf{S}, \quad (5)$$

$$\mathbf{L} = grad\,\mathbf{V} \quad (6)$$

The energy equation

$$(\rho c)_f \frac{d\mathbf{T}}{dt} = k\nabla^2\mathbf{T} + (\rho c)_p\left(D_B \nabla\mathbf{C}\nabla\mathbf{T} + \frac{D_T}{T_0}\nabla\mathbf{T}\nabla\mathbf{T}\right) \quad (7)$$

The nanoparticle volume fraction equation

$$\frac{d\mathbf{C}}{dt} = D_B\nabla^2\mathbf{C} + \frac{D_T}{T_0}\nabla^2\mathbf{T} \quad (8)$$

In the above equations, $\boldsymbol{V}$ is the velocity vector, μ is the dynamic viscosity of the fluid, $\boldsymbol{S}^{\nabla}$ the upper-convected derivative, λ_1 the relaxation times, $\boldsymbol{f}$ is the body force, P is the pressure, ρ_f is density of fluid base, ν is the kinematic viscosity, T is the temperature, D_B is the Brownian diffusion coefficient, D_T is the thermophoretic diffusion coefficient, $\tau = \frac{(\rho c)_p}{(\rho c)_f}$ is the ratio of the effective heat capacity of the nanoparticle material and heat capacity of the fluid with ρ being the density, C is the volumetric volume expansion coefficient and ρ_p is the density of the particles.

We seek the velocity field for the two dimensional and two directional flow of the form

$$\mathbf{V} = \left(U(X,Y,t), V(X,Y,t), 0\right)\cdot \quad (9)$$

Introducing a wave frame (x,y) moving with velocity c away from the fixed frame (X,Y) by the transformation

$$x = X - ct,\ y = Y,\ u = U - c,\ v = V,\ p(x) = P(X,t) \quad (10)$$

Using Eqs. (9) and (10) in Eqs. (2) to (8) the equations in wave frame becomes

$$\frac{\partial u}{\partial x} + \frac{\partial v}{\partial y} = 0, \quad (11)$$

$$\rho_f\left(u\frac{\partial u}{\partial x} + v\frac{\partial u}{\partial y}\right) = -\frac{\partial p}{\partial x} + \frac{\partial}{\partial x}\left(S_{xx}\right) + \frac{\partial}{\partial y}\left(S_{xy}\right) + \quad (12)$$
$$\rho g\sin\alpha + \rho g\alpha\left(T - T_0\right) + \rho g\alpha\left(C - C_0\right),$$

$$\rho_f\left(u\frac{\partial v}{\partial x} + v\frac{\partial v}{\partial y}\right) = -\frac{\partial p}{\partial y} + \frac{\partial}{\partial x}\left(S_{yx}\right) + \quad (13)$$
$$\frac{\partial}{\partial y}\left(S_{yy}\right) - \rho g\cos\alpha,$$

$$\left(u\frac{\partial T}{\partial x} + v\frac{\partial T}{\partial y}\right) = \alpha\left(\frac{\partial^2 T}{\partial x^2} + \frac{\partial^2 T}{\partial y^2}\right) + \quad (14)$$
$$\tau\left\{D_B\left(\frac{\partial C}{\partial x}\frac{\partial T}{\partial x} + \frac{\partial C}{\partial y}\frac{\partial T}{\partial y}\right)\left(\frac{D_T}{T_0}\right)\left[\left(\frac{\partial T}{\partial x}\right)^2 + \left(\frac{\partial T}{\partial y}\right)^2\right]\right\}$$

$$\left(u\frac{\partial C}{\partial x} + v\frac{\partial C}{\partial y}\right) = D_B\left(\frac{\partial^2 C}{\partial x^2} + \frac{\partial^2 C}{\partial y^2}\right) + \quad (15)$$
$$\left(\frac{D_T}{T_0}\right)\left(\frac{\partial^2 T}{\partial x^2} + \frac{\partial^2 T}{\partial y^2}\right)$$

Where the stresses appearing in the above equations are defined through these equations.

$$2\mu\frac{\partial u}{\partial x} = S_{xx} + \quad (16)$$
$$\lambda_1\left(u\frac{\partial S_{xx}}{\partial x} + v\frac{\partial S_{xx}}{\partial y} - 2\frac{\partial u}{\partial x}S_{xx} - 2\frac{\partial u}{\partial y}S_{xy}\right) +$$
$$\frac{1}{2}\left(\lambda_1 - \mu_1\right)\left(4S_{xx}\frac{\partial u}{\partial x} + 2S_{xy}\left(\frac{\partial u}{\partial y} + \frac{\partial v}{\partial x}\right)\right)$$

$$\mu\left(\frac{\partial u}{\partial y} + \frac{\partial v}{\partial x}\right) = S_{xy} + \quad (17)$$
$$\lambda_1\left(u\frac{\partial S_{xy}}{\partial x} + v\frac{\partial S_{xy}}{\partial y} - \frac{\partial v}{\partial x}S_{xx} - \frac{\partial u}{\partial y}S_{yy}\right) +$$
$$\frac{1}{2}\left(\lambda_1 - \mu_1\right)\left((S_{xx} + S_{xy})\left(\frac{\partial u}{\partial y} + \frac{\partial v}{\partial x}\right)\right)$$

$$2\mu\frac{\partial v}{\partial y} = S_{yy} + \quad (18)$$
$$\lambda_1\left(u\frac{\partial S_{yy}}{\partial x} + v\frac{\partial S_{yy}}{\partial y} - 2\frac{\partial v}{\partial y}S_{yy} - 2\frac{\partial v}{\partial x}S_{xy}\right) +$$
$$\frac{1}{2}\left(\lambda_1 - \mu_1\right)\left(4S_{yy}\frac{\partial v}{\partial y} + 2S_{xy}\left(\frac{\partial u}{\partial y} + \frac{\partial v}{\partial x}\right)\right)$$

Defining the following non-dimensional quantities

$$\bar{x}=\frac{x}{\lambda},\ \bar{y}=\frac{y}{d_1},\ \bar{u}=\frac{u}{c},\ \bar{v}=\frac{v}{c},\ \delta=\frac{d_1}{\lambda}, \tag{19}$$

$$d=\frac{d_2}{d_1},\ \bar{p}=\frac{d_1^2 p}{\mu c\lambda},\ \bar{t}=\frac{ct}{\lambda},\ h_1=\frac{H_1}{d_1},$$

$$h_2=\frac{H_2}{d_2},\ a=\frac{a_1}{d_1},\ b=\frac{b_1}{d_1},\ Re=\frac{cd_1}{\nu},\ \bar{\Psi}=\frac{\Psi}{cd_1},$$

$$\theta=\frac{T-T_0}{T_1-T_0},\ \bar{S}_{\bar{x}\bar{x}}=\frac{d_1}{\mu c}S_{xx},\bar{S}_{\bar{x}\bar{y}}=\frac{d_1}{\mu c}S_{xy},$$

$$\bar{S}_{\bar{y}\bar{y}}=\frac{d_1}{\mu c}S_{yy},\ Pr=\frac{\nu}{\alpha},\ N_T=\frac{\tau D_T\left(T_1-T_0\right)}{T_0\nu},$$

$$N_b=\frac{\tau D_B\left(C_1-C_0\right)}{\upsilon},Gr=\frac{\rho g\alpha d_1^2\left(T_1-T_0\right)}{\mu c},$$

$$Br=\frac{\rho g\alpha d_1^2\left(C_1-C_0\right)}{\mu c},\quad Le=\frac{\upsilon}{D_B},$$

With the help of Eq. (19), Eqs. (11) to (18) along with velocity stream function Ψ relation $(u=\frac{\partial\Psi}{\partial y}, v=-\delta\frac{\partial\Psi}{\partial x})$ after dropping the bars take the form

$$Re\delta\left(\Psi_y\Psi_{xy}-\Psi_x\Psi_{yy}\right)=-\frac{\partial p}{\partial x}+\delta\frac{\partial}{\partial x}\left(S_{xx}\right)+ \tag{20}$$
$$\frac{\partial}{\partial y}\left(S_{xy}\right)+Gr\theta+B_r\Phi+\frac{Re}{Fr}\sin\beta,$$

$$Re\delta^3\left(\Psi_x\Psi_{xy}-\Psi_y\Psi_{xx}\right)=-\frac{\partial p}{\partial y}+\delta^2\frac{\partial}{\partial x}\left(S_{xy}\right)+ \tag{21}$$
$$\delta\frac{\partial}{\partial y}\left(S_{yy}\right)-\delta\frac{Re}{Fr}\cos\beta$$

$$Re\delta\left(\Psi_y\theta_x-\Psi_x\theta_y\right)=\frac{1}{Pr}\left(\theta_{yy}+\delta^2\theta_{xx}\right)+ \tag{22}$$
$$N_b\left(\delta^2\theta_x\Phi_x+\theta_y\Phi_y\right)+N_T\left(\delta^2\left(\theta_x\right)^2+\left(\theta_y\right)^2\right)$$

$$Re\delta Le\left(\Psi_y\Phi_x-\Psi_x\Phi_y\right)=\left(\Phi_{yy}+\delta^2\Phi_{xx}\right)+ \tag{23}$$
$$\delta^2\frac{N_T}{N_b}\theta_{xx}+\frac{N_T}{N_b}\theta_{yy}$$

Where

$$2\delta\Psi_{xy}=S_{xx}+ \tag{24}$$
$$\lambda_1\left(\delta\left(\Psi_y\frac{\partial}{\partial x}-\Psi_x\frac{\partial}{\partial y}\right)S_{xx}-2\delta\Psi_{xy}S_{xx}-2\Psi_{yy}S_{xy}\right)+$$
$$\frac{1}{2}\left(\lambda_1-\mu_1\right)\left(4\delta\Psi_{xy}S_{xx}+2\left(\Psi_{yy}-\delta^2\Psi_{xx}\right)S_{xy}\right)$$

$$\Psi_{yy}-\delta^2\Psi_{xx}=S_{xy}+ \tag{25}$$
$$\lambda_1\left(\delta\left(\Psi_y\frac{\partial}{\partial x}-\Psi_x\frac{\partial}{\partial y}\right)S_{xy}+\delta^2\Psi_{xx}S_{xx}-\Psi_{yy}S_{yy}\right)+$$
$$\frac{1}{2}\left(\lambda_1-\mu_1\right)\left(\left(\Psi_{yy}-\delta^2\Psi_{xx}\right)\left(S_{xx}+S_{yy}\right)\right)$$

$$-2\delta\Psi_{xy}=S_{yy}+ \tag{26}$$
$$\lambda_1\left(\delta\left(\Psi_y\frac{\partial}{\partial x}-\Psi_x\frac{\partial}{\partial y}\right)S_{yy}+2\delta^2\Psi_{xx}S_{xy}+2\delta\Psi_{xy}S_{yy}\right)+$$
$$\frac{1}{2}\left(\lambda_1-\mu_1\right)\left(2\left(\Psi_{yy}-\delta^2\Psi_{xx}\right)S_{xy}-4\delta\Psi_{xy}S_{yy}\right)$$

The corresponding boundary conditions in terms of stream function are defined as

$$\Psi=\frac{q}{2}\ \text{at}\ y=h_1=1+a\cos2\pi x, \tag{27}$$
$$\Psi=-\frac{q}{2}\ \text{at}\ y=h_2=-d-b\cos(2\pi x+\varphi),$$
$$\frac{\partial\Psi}{\partial y}=-1\ \text{at}\ y=h_1\ \text{and}\ y=h_2,$$

$$\theta=0\ \text{at}\ y=h_1, \tag{28}$$
$$\theta=1\ \text{at}\ y=h_2,$$

$$\Phi=0\ \text{at}\ y=h_1, \tag{29}$$
$$\Phi=1\ \text{at}\ y=h_2$$

Where q is the flux in the wave frame, a, b, ϕ and d satisfy the relation

$$a^2+b^2+2ab\cos\varphi\le(1+d)^2.$$

Under the assumption of long wave length $\delta \ll 1$ and low Reynolds number, Eqs. (20) to (26) become

$$\frac{\partial p}{\partial x}=\frac{\partial S_{xy}}{\partial y}+\frac{Re}{Fr}\sin\beta+Gr\theta+B_r\Phi, \tag{30}$$

$$\frac{\partial p}{\partial y}=0, \tag{31}$$

$$\frac{1}{Pr}\frac{\partial^2\theta}{\partial y^2}+N_b\frac{\partial\theta}{\partial y}\frac{\partial\Phi}{\partial y}+N_t\left(\frac{\partial\theta}{\partial y}\right)^2=0, \tag{32}$$

$$\frac{\partial^2\Phi}{\partial y^2}+\frac{N_t}{N_b}\frac{\partial^2\theta}{\partial y^2}=0 \tag{33}$$

$$S_{xx}=\left(\lambda_1+\mu_1\right)S_{xy}\Psi_{yy}, \tag{34}$$

$$S_{xy}=\frac{\Psi_{yy}}{1+\zeta\Psi_{yy}^2}, \tag{35}$$

$$S_{yy}=\left(-\lambda_1+\mu_1\right)S_{xy}\Psi_{yy}, \tag{36}$$

Where $\zeta=\lambda_1^2+\frac{\lambda_1^2-\mu_1^2}{2}$.

Elimination of pressure from Eqs. (30) and (31), yields

$$\frac{\partial^2}{\partial y^2}\left(\frac{\Psi_{yy}}{1+\zeta\Psi_{yy}^2}\right)+Gr\frac{\partial\theta}{\partial y}+B_r\frac{\partial\Phi}{\partial y}=0 \tag{37}$$

The above equation can also be written as

$$\frac{\partial^4\Psi}{\partial y^4}-\zeta\frac{\partial^2}{\partial y^2}\left(\frac{\partial^2\Psi}{\partial y^2}\right)^3+Gr\frac{\partial\theta}{\partial y}+B_r\frac{\partial\Phi}{\partial y}=0 \tag{38}$$

Solution of the problem

In order to calculate the solutions for the given system of linear and non-linear differential equations, the treasured solution for Eq. (33) is defined as

$$\Phi(x,y)=-\frac{N_t}{N_b}\theta+a_1(x)y+a_2(x) \tag{39}$$

Where $a_1(x)$ and $a_2(x)$ are unknown functions. Now substitute Eq. (39) into (32) we get

$$\frac{\partial^2\theta}{\partial y^2}+Pr\,N_b a_1(x)\frac{\partial\theta}{\partial y}=0 \tag{40}$$

The exact solution of Eq. (40) give the temperature distribution as

$$\theta(x,y)=\frac{a_3(x)}{Pr\,N_b a_1(x)}+a_4(x)e^{-a_1(x)Pr\,N_b y} \tag{41}$$

Where $a_3(x)$ and $a_4(x)$ are unknown functions. Now with the help of temperature distribution (Eq. (41)), the nano-particle concentration Φ is given from Eq. (39) as:

$$\Phi(x,y)=-\frac{N_t}{N_b}\left(\frac{a_3(x)}{Pr\,N_b a_1(x)}+a_4(x)e^{-a_1(x)Pr\,N_b y}\right)+ \tag{42}$$

$$a_1(x)y+a_2(x)$$

By applying the boundary conditions, values of unknown functions $a_1(x)$, $a_2(x)$, $a_3(x)$ and $a_4(x)$ are defined as

$$a_1(x)=\frac{1+\frac{N_t}{N_b}}{h_2-h_1}, \tag{43}$$

$$a_2(x)=-h_1\left(\frac{1+\frac{N_t}{N_b}}{h_2-h_1}\right),$$

$$a_3(x)=-Pr\,N_b a_1(x)\left(\frac{e^{-a_1(x)Pr\,N_b h_1}}{e^{-a_1(x)Pr\,N_b h_2}-e^{-a_1(x)Pr\,N_b h_1}}\right)$$

$$a_4(x)=\frac{1}{e^{-a_1(x)Pr\,N_b h_2}-e^{-a_1(x)Pr\,N_b h_1}}$$

Thus the exact expressions for the temperature distribution θ and nano-particle concentration Φ are given by

$$\theta(x,y)=\frac{e^{-a_1(x)Pr\,N_b y}-e^{-a_1(x)Pr\,N_b h_1}}{e^{-a_1(x)Pr\,N_b h_2}-e^{-a_1(x)Pr\,N_b h_1}} \tag{44}$$

$$\Phi(x,y)=\left(1+\frac{N_t}{N_b}\right)\left(\frac{y-h_1}{h_2-h_1}\right)- \tag{45}$$

$$\frac{N_t}{N_b}\left(\frac{e^{-a_1(x)Pr\,N_b y}-e^{-a_1(x)Pr\,N_b h_1}}{e^{-a_1(x)Pr\,N_b h_2}-e^{-a_1(x)Pr\,N_b h_1}}\right)$$

Eqs. (30) and (38) are highly non-linear equations, so the exact solutions are looking difficult, Therefore,

we apply regular perturbation technique. Now we expand Ψ, p and q as:

$$\Psi=\Psi_0+\zeta(\Psi_1),\quad p=p_0+\zeta(p_1),\quad q=q_0+\zeta(q_1) \tag{46}$$

Substituting Eq. (41) into Eqs. (29) and (37) and then solving the resulting zeroth and first order systems and setting $q_0=q-\zeta q_1$, we arrive at

$$\Psi=\frac{1}{24k_0^4(h_1-h_2)^3}\times \tag{47}$$
$$\left(k_0^4(h_1-h_2)(h_1-y)(h_2-y)\times\right.$$
$$(Brk_2(h_1-h_2)^2(h_1-y)(h_2-y)+24(h_1+h_2-2y))+$$
$$+24k_3k_0(h_1-h_2)(h_1-y)(h_2-y)((h_1-y)e^{h_2k_0}+$$
$$e^{h_1k_0}(h_2-y))+24k_3((h_1-h_2)^3e^{k_0y}+e^{h_1k_0}$$
$$(h_2-y)^2(-3h_1+h_2+2y)+$$
$$\left.(h_1-y)^2e^{h_2k_0}(-h_1+3h_2-2y))\right)-$$
$$\frac{1}{2(h_1-h_2)^3}\left(q(h_1+h_2-2y)\right.$$
$$\left.(h_1^2+2y(h_1+h_2)-4h_1h_2+h_2^2-2y^2)\right)+$$
$$\zeta\left(\frac{b_{00}y^3+3y\left(b_{01}y+b_{02}\right)+b_{03}}{45360k_0^8(h_1-h_2)^3}+\right.$$
$$\frac{1}{45360k_0^8}\left(14175k_0^2e^{k_0y}(384k_8y^2+k_9e^{k_0y}+\right.$$
$$64\left(3k_{14}y+k_{13}\right))-5670k_0^3e^{k_0y}(128k_8y^3+$$
$$96k_{14}y^2+2k_9ye^{k_0y}+64k_{13}y+k_{17}e^{k_0y}+32k_{12})+$$
$$9k_0^8y^4(y(3k_6y^3+6k_5y^2+14k_7y+42k_{16})+210k_4)+$$
$$35k_0^4e^{k_0y}(1296k_8y^4+1296k_{14}y^3+81k_9y^2e^{k_0y}+$$
$$1296k_{13}y^2+1296k_{12}y+81k_{17}ye^{k_0y}+16k_{10}e^{2k_0y}+$$
$$81k_{15}e^{k_0y}+1296k_{11})-5443200k_0e^{k_0y}\left(4k_8y+k_{14}\right)+$$
$$\left.38102400k_8e^{k_0y}\right)),$$

$$\frac{dp}{dx}=Br\left(\frac{\left(y-h_1\right)\left(\frac{N_t}{N_b}+1\right)}{h_2-h_1}-\right. \tag{48}$$
$$\left.\frac{N_t\left(e^{-a_1(x)PrN_by}-e^{-a_1(x)h_1PrN_b}\right)}{N_b\left(e^{-a_1(x)h_2PrN_b}-e^{-a_1(x)h_1PrN_b}\right)}\right)+6b_{05}+Brk_2y+$$
$$\frac{k_3e^{k_0y}}{k_0}+Gr\left(\frac{e^{-a_1(x)PrN_by}-e^{-a_1(x)h_1Pr)N_b}}{e^{-a_1(x)h_2PrN_b}-e^{-a_1(x)h_1Pr)N_b}}\right)+\frac{Re}{Fr}\sin\beta+$$
$$\xi(b_{04}^2(-72b_{05}-12Brk_2y-\frac{12k_3e^{k_0y}}{k_0})-$$
$$\frac{6b_{04}\left(k_0\left(6b_{05}+Brk_2y\right)+k_3e^{k_0y}\right)}{k_0^3}\times$$
$$\frac{\left(k_0^2y\left(12b_{05}+Brk_2y\right)+2k_3e^{k_0y}\right)}{k_0^3}+\frac{1}{7560k_0^8}\times$$
$$(126k_0^3(-15e^{k_0y}(72b_{05}Brk_2k_3k_0^3y^2\left(k_0y+3\right)+$$
$$432b_{05}^2k_3k_0^3y\left(k_0y+2\right)+k_0(k_0^3(3Br^2k_2^2k_3y^4-$$
$$4(y(y(y\left(k_8y+k_{14}\right)$$

$$\Delta p=\int_0^1\left(\frac{dp}{dx}\right)|_{y=0}, \tag{49}$$

Where the constants appearing in Eqs. (47) and (48) are defined in appendix.

Expressions for different wave shape

The non- dimensional expressions for five considered wave form are given by [26]. The expressions for the triangular, square and trapezoidal wave are derived from the Fourier series.

1) Sinusoidal wave

$$h_1(x)=1+a\sin2\pi x,\quad h_2(x)=-d-b\sin(2\pi x+\varphi).$$

2) Multisinusoidal wave

$$h_1(x)=1+a\sin2n\pi x,\quad h_2(x)=-d-b\sin(2n\pi x+\varphi).$$

3) Triangular wave

$$h_1(x)=1+a\left[\frac{8}{\pi^3}\sum_{m=1}^{\infty}\frac{(-1)^{m+1}}{(2m-1)^2}\sin\left(2\pi(2m-1)x\right)\right],$$

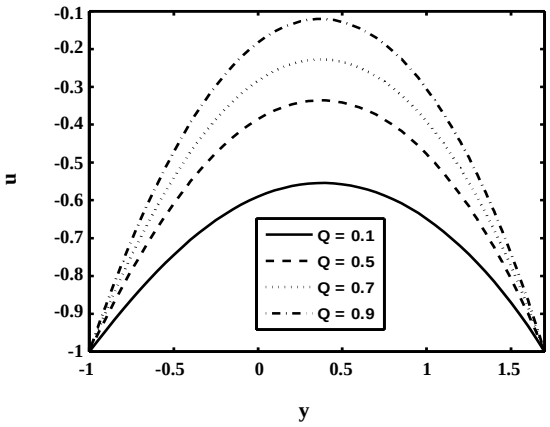

Fig. 1: Velocity profile for different values of Q for fixed values of a= 0.7, b= 0.7, d= 1, ϕ= π/2, Gr= 0.8, N_b= 0.5, Pr= 2, N_t= 0.9, x= 0, Br= 0.6, ξ= 0.08.

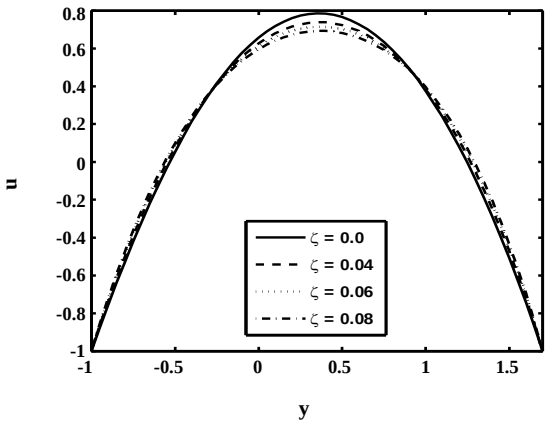

Fig. 2: Velocity profile for different values of ξ for fixed values of a= 0.7, b= 0.7, d= 1, ϕ= π/2, Gr= 0.8, N_b= 0.5, Pr= 2, N_t= 0.9, x= 0, Br= 0.6, Q= 0.08.

$$h_2(x) = -d - b\left[\frac{8}{\pi^3}\sum_{m=1}^{\infty}\frac{(-1)^{m+1}}{(2m-1)^2}\sin\left(2\pi(2m-1)x+\varphi\right)\right].$$

4) Trapezoidal wave

$$h_1(x) = 1 + a\left[\frac{32}{\pi^2}\sum_{m=1}^{\infty}\frac{\sin\frac{\pi}{8}(2m-1)}{(2m-1)^2}\sin\left(2\pi(2m-1)x\right)\right],$$

$$h_2(x) = -d - b\left[\frac{32}{\pi^2}\sum_{m=1}^{\infty}\frac{\sin\frac{\pi}{8}(2m-1)}{(2m-1)^2}\sin\left(2\pi(2m-1)x+\varphi\right)\right].$$

5) Square wave

$$h_1(x) = 1 + a\left[\frac{4}{\pi}\sum_{m=1}^{\infty}\frac{(-1)^{m+1}}{(2m-1)}\cos\left(2(2m-1)\pi x\right)\right],$$

$$h_2(x) = -d - b\left[\frac{4}{\pi}\sum_{m=1}^{\infty}\frac{(-1)^{m+1}}{(2m-1)}\cos\left(2(2m-1)\pi x+\varphi\right)\right].$$

Numerical results and discussion

The main objective of this portion is to revise the graphical significances of the present flow problem. Mathematica software is used to carry out the expressions for pressure rise and pressure gradient because pressure rise definition involves integration of dp/dx which is not solvable analytically. Figs. 1 to 3 show the velocity profile for different values of volume flow rate Q, pseudoplastic parameter ξ and different wave forms. It is observed from Fig. 1 that the magnitude value of the velocity profile decreases with an increase in Q. Fig. 2 shows the velocity profile for different values of ξ. It is depicted from Fig. 2 that near the center of the channel the magnitude of the velocity profile decreases with an increase in ξ Fig. 3 shows the velocity profile for different wave forms. It is observed from Fig. 3 that the magnitude value of the velocity profile increases in sinusoidal, multisinsoidal, trapezoidal and triangular wave. In order to see the behavior of pressure rise for different values of β, Gr, d and ξ Figs. 4 to 7 are prepared. It is observed from Figs. 4 and 5 that the behavior of pressure rise in augmented pumping $(\Delta p<0,\ Q>0)$, peristaltic pumping $(\Delta p>0,\ Q>0)$ and retrograde pumping $(\Delta p>0,\ Q<0)$ regions is same. In these regions the pressure rise increases with an increase in β and Gr. It is depicted from Figs. 6 and 7 that in the augmented pumping region $(\Delta p<0,\ Q>0)$ the pressure rise increases with an increase in the width of the channel d, while in the peristaltic pumping $(\Delta p>0,\ Q>0)$ region the pressure rise decreases. Figs. 8 to 10 indicate the pressure gradient for different value of Fr and ξ. It is depicted that for $x\in[0,0.2]$ and $x\in[0.8,1]$, the pressure gradient is small i.e., the flow can easily pass with out imposition of a large pressure gradient, while in the region $x\in[0.2,0.8]$, pressure gradient decreases with an increase in Fr and ξ, large

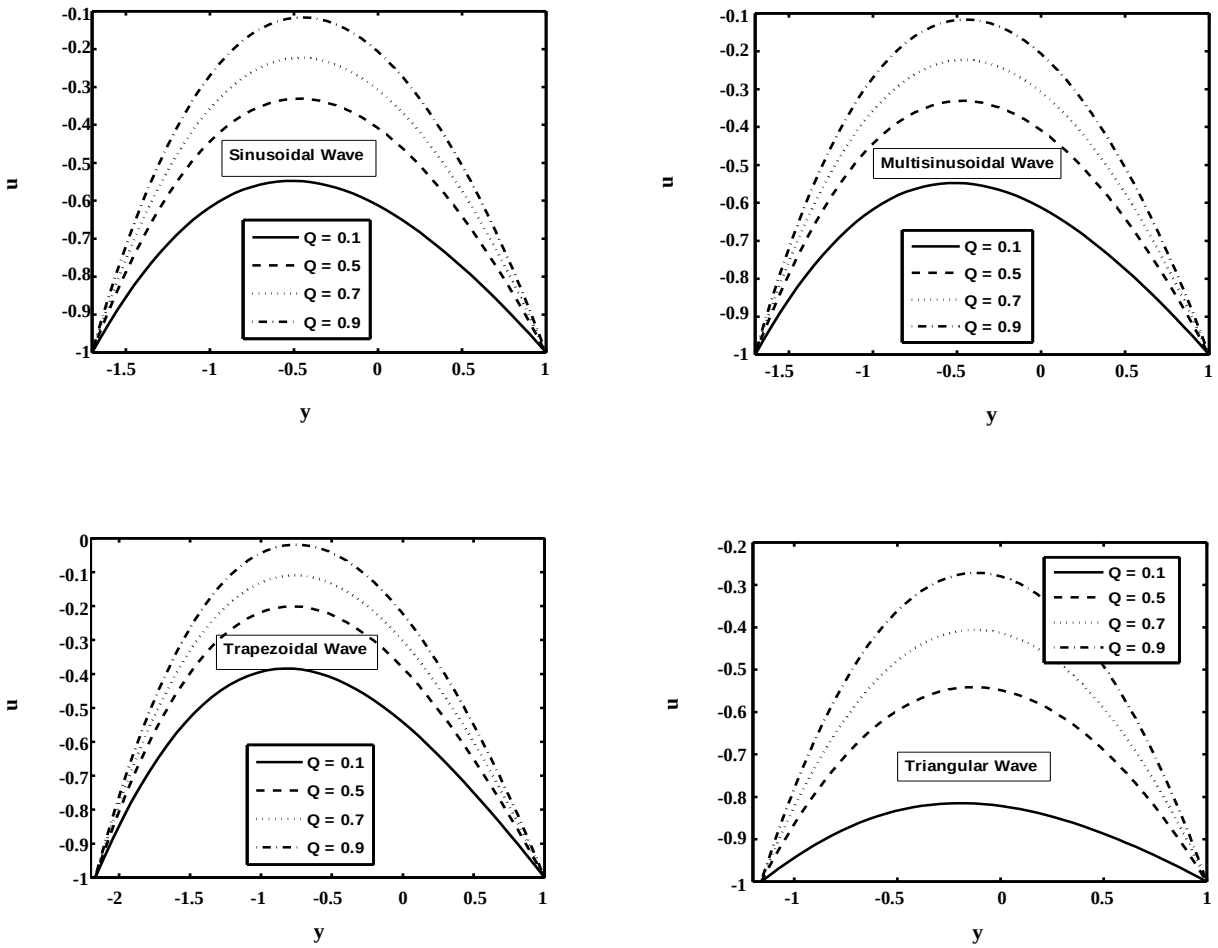

Fig. 3: Velocity profile for different wave forms for fixed values of a= 0.7, b= 0.7, d= 1, ϕ= π/2, Gr= 0.8, N_b= 0.5, Pr= 2, N_t= 0.9, x=0, Br= 0.6, ξ= 0.08. (a) for sinusoidal wave, (b) for multisinusoidal wave, (c) for Trapezoidal wave, (d) for Triangular wave.

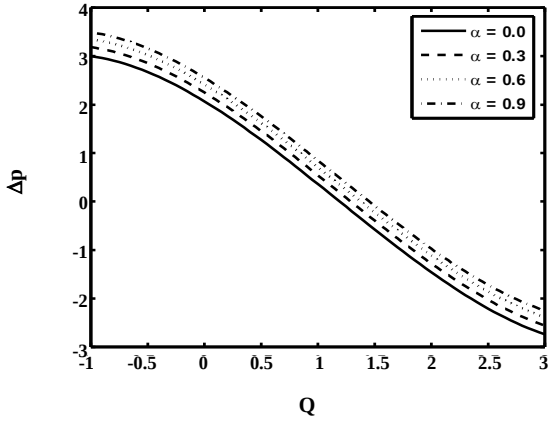

Fig. 4: Variation of pressure rise Δp with Q for a= 0.7, b= 0.7, d= 1.5, ϕ= π/2, ξ= 0.01, N_t= 0.9, N_b= 0.5, Pr= 1, Gr= 0.8, Br= 0.9, Re= 0.5, Fr= 0.8.

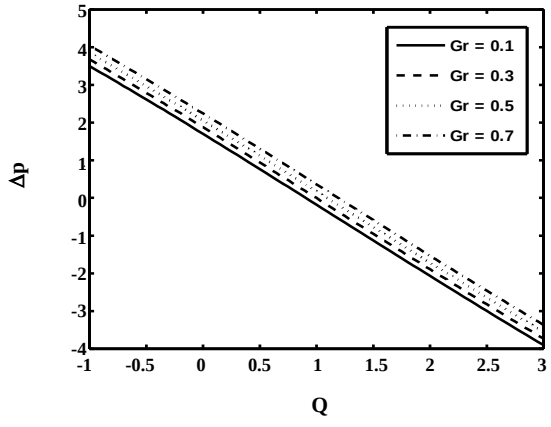

Fig. 5: Variation of pressure rise Δp with Q for a= 0.7, b= 0.7, α= 0.2, ϕ= π/4, ξ= 0.001, N_t= 0.9, N_b= 0.5, Pr= 1.8, d= 1.5, Br= 0.9, Re= 0.5, Fr= 0.8.

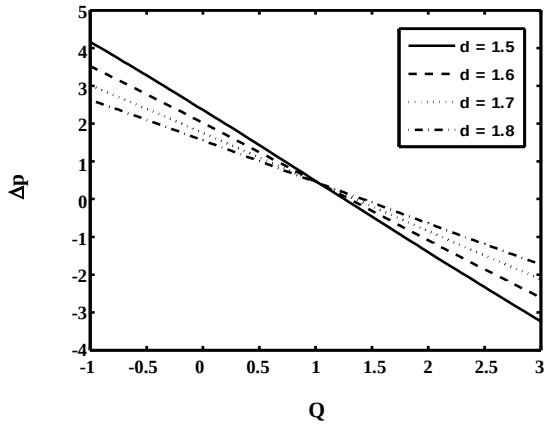

Fig. 6: Variation of pressure rise Δp with Q for a=0.7, b=0.7, α= 0.2, ϕ= π/4, ξ= 0.001, N_t= 0.9, N_b= 0.5, Pr= 1, Gr= 0.8, Br= 0.9, Re=0.5, Fr= 0.8.

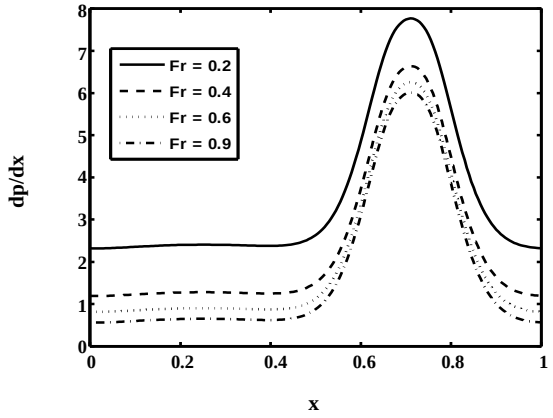

Fig. 8: Variation of pressure gradient dp/dx with X for a= 0.7, b= 0.7, α= 0.6, ϕ= π/6, ξ= 0.03, Q= 0.5, N_t= 0.9, N_b= 0.5, Pr= 1.5, d= 1.5, Br= 0.9, Re= 0.8, Gr= 0.8.

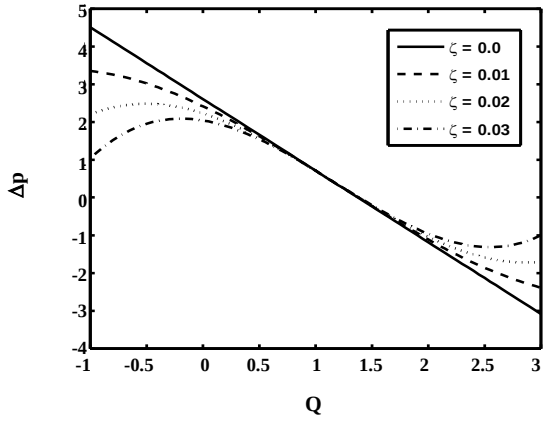

Fig. 7: Variation of pressure rise Δp with Q for a=0.7, b= 0.7, α= 0.2, ϕ= π/4, Gr= 0.8, N_t= 0.9, N_b= 0.5, Pr= 1, d= 1.5, Br= 0.9, Re=0.5, Fr= 0.8.

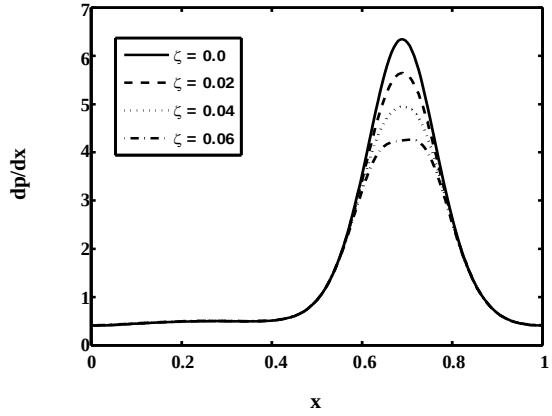

Fig. 9: Variation of pressure gradient dp/dx with X for a= 0.7, b= 0.7, α= 0.6, ϕ= π/4, Fr= 0.8, Q= 0.5, N_t= 0.9, N_b= 0.5, Pr= 1.5, d= 1.5, Br= 0.9, Re= 0.5, Gr= 0.8.

amount of pressure gradient is required to maintain the flux to pass. Figs. 10 indicate the pressure gradient for different wave forms. Figs. 11 and 12 are displayed to analysis the influence of temperature profile on N_t and Pr It is explored from Figs. 11 and 12 that the temperature profile increases with an increase in N_t and Pr. This is physically valid because these parameters show a direct relationship with temperature. To examine the effects of concentration profile on N_t and Pr, Figs. 13 and 14 are prepared. It is illustrated from figures that the concentration profile decreases with an increase in N_t and Pr.

Stream lines for different values of d and ξ are shown in Figs. 15 to 16. It is depicted from Figs. 15 that the size of the trapping bolus decreases with the decrease in the width of the channel. It is observed form Fig. 16 that the size of the trapping bolus increases with an increase in ξ. It is also observed from Figs. 15 and 16 that the trapping bolus also shifted towards right side of the channel and this happens due to increase of phase angle. Stream lines for different wave forms are shown in Fig. 17.

CONCLUSIONS

In the current research paper we have investigated the influence of nanofluid on peristaltic transport of a pseudoplastic fluid in the presence of inclined asymmetric channel. With the help of long wavelength

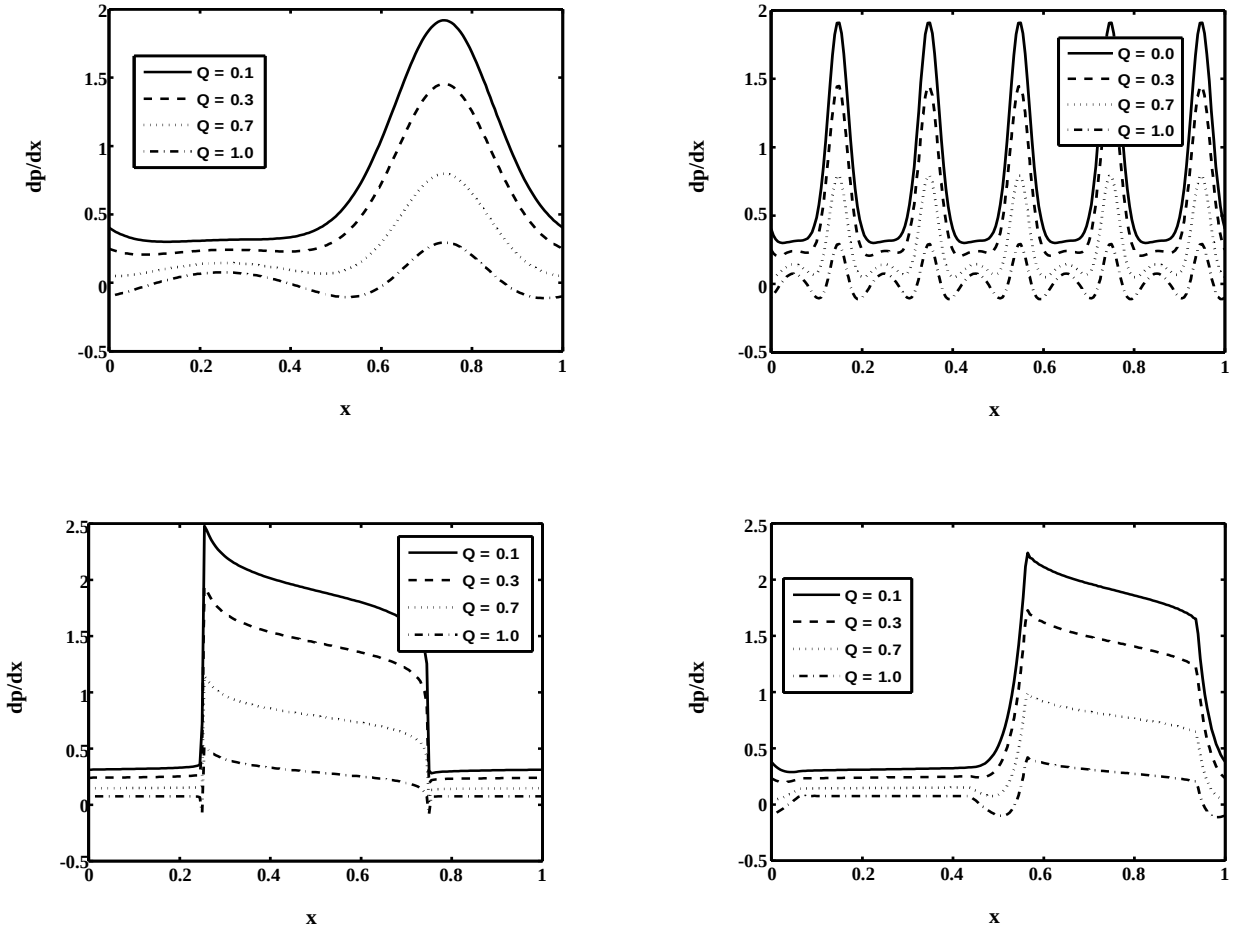

Fig. 10: Variation of pressure gradient dp/dx with x for a= 0.8, b= 0.1, α= 0.6, ϕ= π/4, Fr= 0.8, N_t = 0.9, N_b= 0.5, Pr= 1.0, d= 1.8, Br= 0.9, Re= 0.5, Gr= 0.1, ξ= 0.03. (a) For sinusoidal wave, (b) For multisinusiodal wave, (c) For square wave, (d) For Triangular wave.

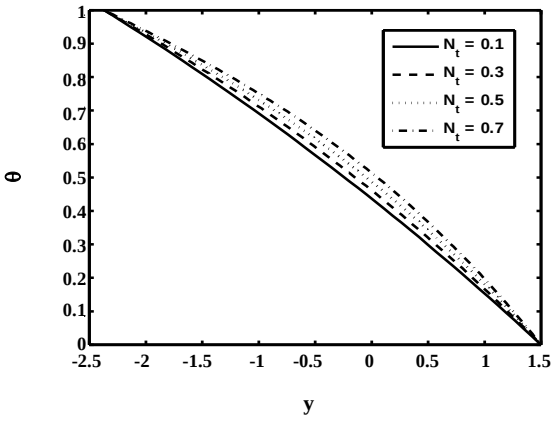

Fig. 11: Temperature profile for different values of N_t for fixed values of a= 0.5, b= 1.0, Pr= 1, N_b= 0.3, d= 1.5, x=0, ϕ= π/6.

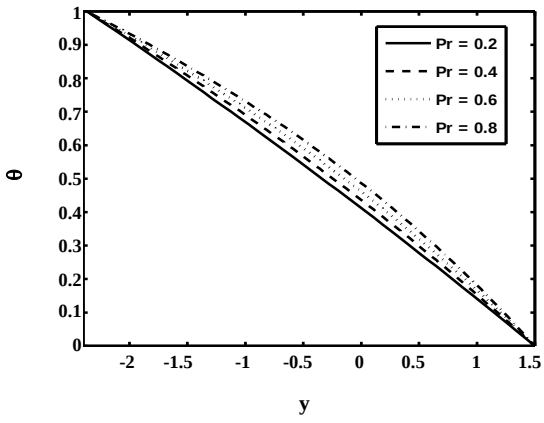

Fig. 12: Temperature profile for different values of Pr for fixed values of a= 0.5, b= 1.0, N_t= 0.7, N_b= 0.3, d= 1.5, x=0, ϕ= π/6.

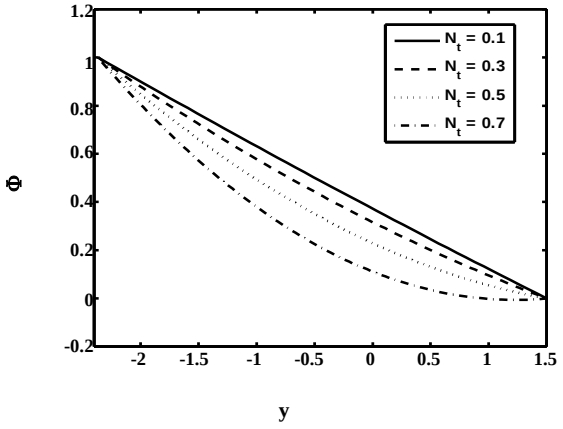

Fig. 13: Concentration profile for different values of N_t for fixed values of a= 0.5, b= 1.0, Pr= 1, N_b= 0.3, d= 1.5, x=0, $\phi = \pi/6$.

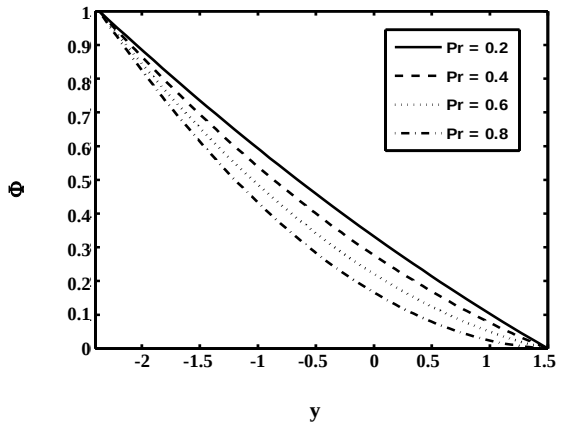

Fig. 14: Concentration profile for different values of Pr for fixed values of a= 0.5, b= 1.0, N_t= 0.7, N_b= 0.3, d= 1.5, x=0, $\phi = \pi/6$.

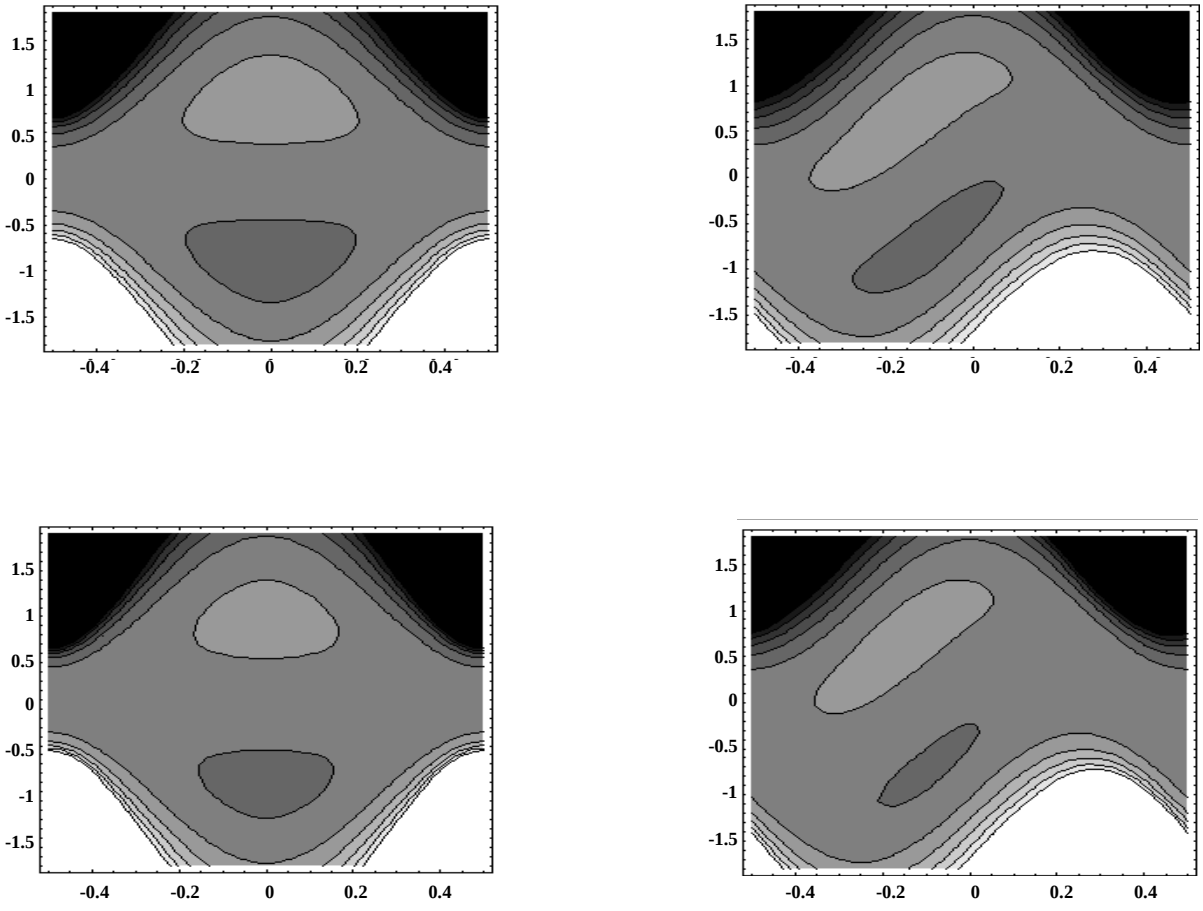

Fig. 15: Stream lines for different values of d and ϕ for fixed values of a= 0.7, b= 0.7, d= 1, N_t= 0.9, N_b= 0.5, Pr= 1, Q= 2, B_r= 0.1, ξ= 0.03, Gr= 0.1.

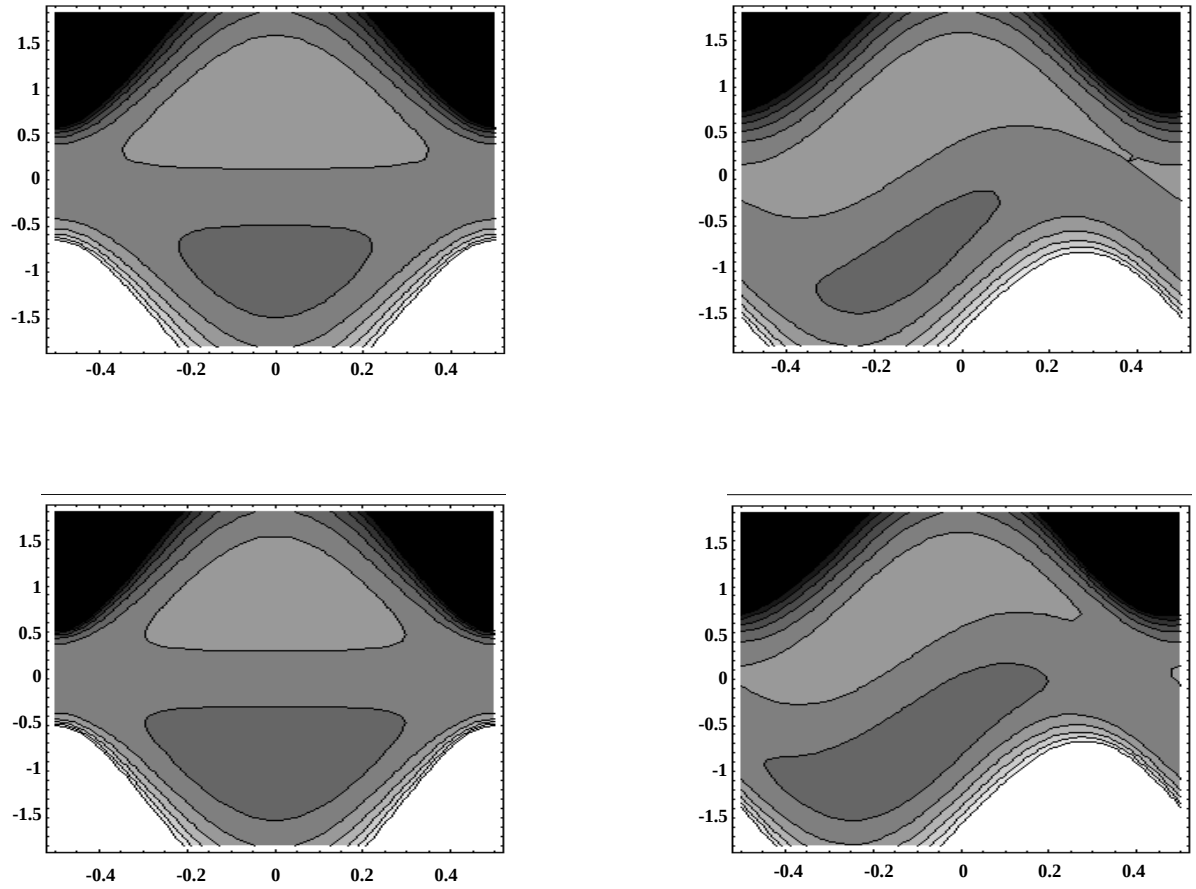

Fig. 16: Stream lines for different values of ξ and ϕ for fixed values of a= 0.7, b= 0.7, d= 1, N_t= 0.9, N_b= 0.5, Pr= 1.5, Q= 1.8, B_r= 0.9, d= 1, Gr= 0.8.

and low Reynolds number approximation the governing equations of a pseudoplastic fluid along with nanofluid are modeled. The exact solutions for temperature and nano particle volume fraction are calculated. Perturbation technique is used to carry out the series solution of stream function and pressure gradient. Graphical results were plotted and reported for different involved physical parameters of interest. The main results of the present study can be summarized as follows:

- The magnitude value of the velocity profile decreases with an increase in Q and ζ
- The magnitude value of the velocity profile increases in sinusoidal, multisinsoidal, trapezoidal and triangular waves.
- The pressure gradient decreases with an increase in Fr and ξ.
- The temperature profile increases with an increase in N_t and Pr.
- The concentration profile decreases with an increase in N_t and Pr.
- The size of the trapping bolus decreases with the decrease in the width of the channel d and increases with an increase in ξ.

Appendix

$$k_0 = -a_1(x)\,Pr\,N_b,$$

$$k_1 = \frac{k_0}{e^{h_2 k_0} - e^{h_1 k_0}},$$

$$k_2 = \frac{\frac{N_t}{N_b} + 1}{h_2 - h_1},$$

$$k_3 = \frac{Br k_1 N_t}{N_b} - Gr k_1,$$

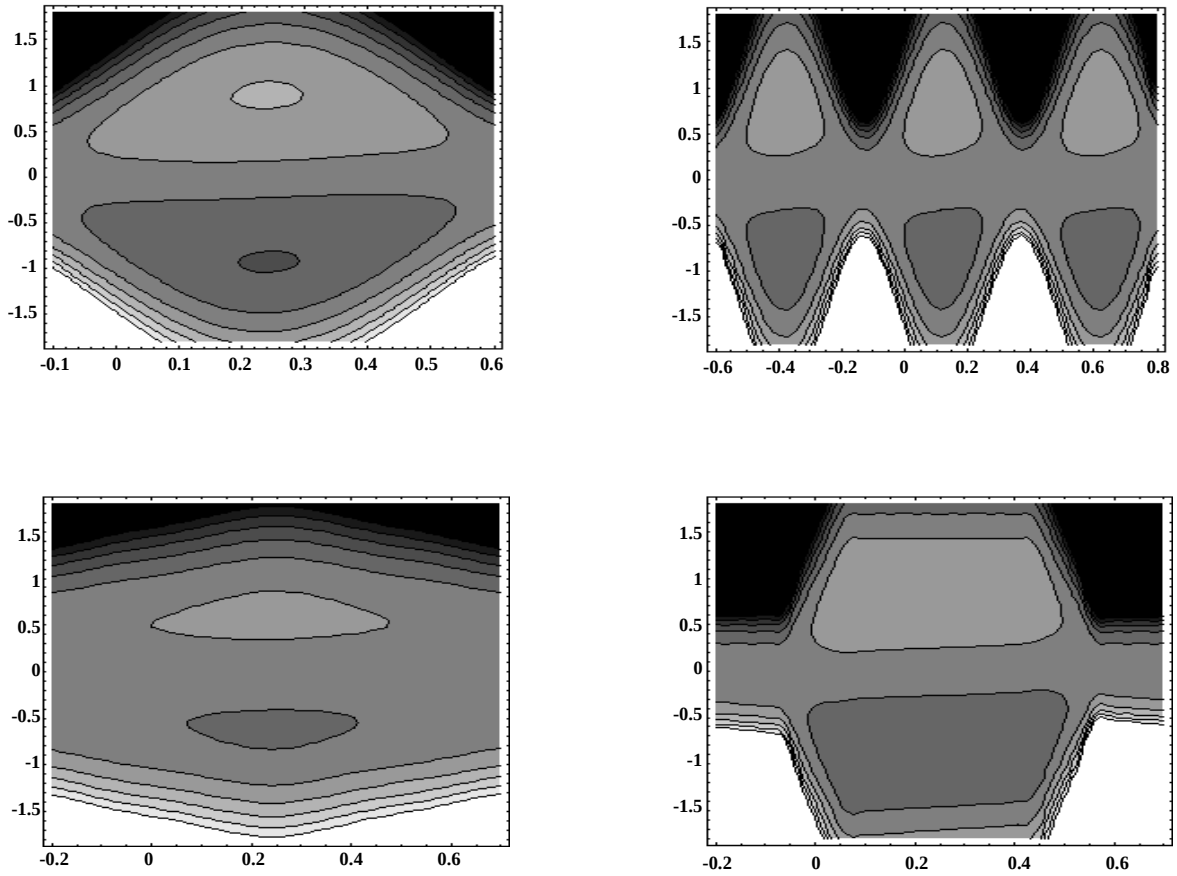

Fig. 17: Stream lines for different wave forms for fixed values of a= 0.7, b= 0.7, d= 1, N_t= 0.9, N_b= 0.5, Pr= 1.5, Q= 1.8, B_r= 0.9, d= 1, Gr= 0.8.

$$k_4 = 12b_{04}^2 Brk_2 + 432b_{05}^2 b_{04},$$

$$k_5 = 90b_{05} Br^2 k_2^2,$$

$$k_6 = \frac{15}{4} Br^3 k_2^3,$$

$$k_7 = 18b_{04} Br^2 k_2^2 + 648b_{05}^2 Brk_2,$$

$$k_8 = \frac{3}{4} Br^2 k_2^2 k_3,$$

$$k_9 = \frac{6Brk_2 k_3^2}{k_0^2},$$

$$k_{10} = \frac{9k_3^3}{k_0^4},$$

$$k_{11} = \frac{12b_{04} Brk_2 k_3}{k_0^2} + 12b_{04}^2 k_3 + \frac{144b_{05} b_{04} k_3}{k_0} + \frac{216b_{05}^2 k_3}{k_0^2},$$

$$k_{12} = \frac{108b_{05} Brk_2 k_3}{k_0^2} + \frac{24b_{04} Brk_2 k_3}{k_0} + \frac{432b_{05}^2 k_3}{k_0} + 72b_{04} b_{05} k_3,$$

$$k_{13} = \frac{108b_{05} Brk_2 k_3}{k_0} + 6b_{04} Brk_2 k_3 + 108b_{05}^2 k_3 + \frac{9Br^2 k_2^2 k_3}{k_0^2},$$

$$k_{14}=18b_{05}Brk_3k_2+\frac{6Br^2k_3k_2^2}{k_0},$$

$$k_{15}=\frac{24b_{04}k_3^2}{k_0^2}+\frac{72b_{05}k_3^2}{k_0^3}+\frac{3Brk_2k_3^2}{k_0^4},$$

$$k_{16}=216b_{04}b_{05}Brk_2+1296b_{05}^3,$$

$$k_{17}=\frac{72b_{05}k_3^2}{k_0^2}+\frac{12Brk_2k_3^2}{k_0^3},$$

$$k_{18}=76204800k_8(e^{h_1k_0}-e^{h_2k_0})-$$
$$5443200k_0(e^{h_1k_0}(k_8(11h_1-3h_2)+2k_{14})+$$
$$e^{h_2k_0}(k_8(3h_1-11h_2)-2k_{14})),$$

$$k_{19}=28350k_0^2(32e^{h_1k_0}(12h_1k_8(2h_1-h_2)+$$
$$3k_{14}(3h_1-h_2)+2k_{13})-32e^{h_2k_0}(-12h_2k_8(h_1-2h_2)-$$
$$3k_{14}(h_1-3h_2)+2k_{13})+k_9e^{2h_1k_0}-k_9e^{2h_2k_0}),$$

$$k_{20}=18k_0^8((h_1-h_2)^3(21k_{16}(3h_1^2+4h_1h_2+3h_2^2)+$$
$$3k_5(5h_1^4+8h_1^3h_2+9h_1^2h_2+8h_1^3h_2+5h_2^4)+$$
$$(h_1+h_2)(14k_7(2h_1^2+h_1h_2+2h2^2)+$$
$$3k_6(3h_1^4+2h_1^3h_2+2h_1h_2^3+3h_2^4)+210k_4(h_1+h_2))),$$

$$k_{21}=5670k_0^3(-32e^{h_1k_0}(2h_1^2k_8(13h_1-9h_2)+$$
$$3h_1k_{14}(5h_1-3h_2)+k_{13}(7h_1-3h_2)+2k_{12})+$$
$$32e^{h_2k_0}(2h_2^2k_8(13h_2-9h_1)+3h_2k_{14}(5h_2-3h_1)+$$
$$k_{13}(7h_2-3h_1)+2k_{12})+e^{2h_2k_0}(k_9(7h_2-3h_1)+2k_{17})+$$
$$e^{2h_1k_0}(k_9(3h_2-7h_1)-2k_{17}))),$$

$$k_{22}=1296e^{h_1k_0}(2h_1^3k_8(7h_1-6h_2)+$$
$$h_1(k_{13}(8h_1-6h_2)+h_1k_{14}(11h_1-9h_2))+$$
$$k_{12}(5h_1-3h_2)+2k_{11})+32k_{10}e^{3h_1k_0}-32k_{10}e^{3h_2k_0},$$

$$k_{23}=35k_0^4(-1296e^{h_2k_0}(2h_2^3k_8(7h_2-6h_1)+$$
$$h_2(k_{13}(8h_2-6h_1)+h_2k_{14}(11h_2-9h_1))+$$
$$k_{12}(5h_2-3h_1)+2k_{11})-81e^{2h_2k_0}(2h_2k_9(4h_2-3h_1)+$$
$$k_{17}(5h_2-3h_1)+2k_{15})+81e^{2h_1k_0}(2h_1k_9(4h_1-3h_2)+$$
$$k_{17}(5h_1-3h_2)+2k_{15})+k_{22}),$$

$$k_{24}=210k_0^5(h_1-h_2)(-8k_{10}e^{3h_1k_0}-$$
$$216e^{h_1k_0}(h_1(h_1(h_1(h_1k_8+k_{14})+k_{13})+k_{12})+k_{11})-$$
$$27e^{2h_1k_0}\left(h_1\left(h_1k_9+k_{17}\right)+k_{15}\right)-8k_{10}e^{3h_2k_0}-$$
$$216e^{h_2k_0}(h_2(h_2(h_2\left(h_2k_8+k_{14}\right)+k_{13})+k_{12})+k_{11})-$$
$$27e^{2h_2k_0}\left(h_2\left(h_2k_9+k_{17}\right)+k_{15}\right)),$$

$$k_{25}=-38102400k_8(h_1+h_2)\left(e^{h_1k_0}-e^{h_2k_0}\right),$$

$$k_{26}=5443200k_0(e^{h_1k_0}\left(k_8\left(5h_1^2+5h_1h_2-2h_2^2\right)+\right.$$
$$\left.k_{14}(h_1+h_2)\right)-e^{h_2k_0}k_8(-2h_1^2+5h_1h_2+5h_2^2)+$$
$$k_{14}(h_1+h_2))),$$

$$k_{27}=14175k_0^2(-64e^{h_1k_0}(2h_1k_8(5h_1^2+5h_1h_2-4h_2^2)+$$
$$2k_{14}(2h_1^2+2h_1h_2-h_2^2)+k_{13}(h_1+h_2))+$$
$$64e^{h_2k_0}(2h_2k_8(-4h_1^2+5h_1h_2+5h_2^2)-$$
$$2k_{14}(h_1^2-2h_1h_2-2h_2^2)+k_{13}(h_1+h_2))$$
$$+k_9(h_1+h_2)e^{2h_2k_0}-k_9(h_1+h_2)e^{2h_1k_0}),$$

$$k_{28}=70k_4\left(h_1^2+4h_1h_2+h_2^2\right)(h_1-h_2)^3,$$

$$k_{29}=(h_1-h_2)^3(14(h_1^2+3h_1h_2+h_2^2)(k_7(h1+h_1h_2+h_2^2)+$$
$$2k_{16}(h_1+h_2))+4k_5(h_1+h_2)$$
$$(2h_1^4+6h_1^3h_2+5h_1^2h_2^2+6h_{12}^3h_2+2h_2^4)+$$
$$k_6(5h_1^6+20h_1^5h_2+29h_1^4h_2^2+32h_1^3h_2^3+5h_2^6+$$
$$29h_1^2h_2^4+20h_1h_2^5),$$

$$k_{30}=32e^{h_1k_0}(2h_1^2k_8(5h_1^2+5h_1h_2-6h_2^2)+$$
$$6h_1k_{14}(h_1^2+h_1h_2-h_2^2)+k_{13}(3h_1^2+3h_1h_2-2h_2^2)+$$
$$k_{12}(h_1+h_2)),$$

$$k_{31}=2h_2^2k_8(-6h_1^2+5h_1h_2+5h_2^2)+$$
$$6h_2k_{14}(-h_1^2+h_1h_2+h_2^2)+k_{13}(-2h_1^2+3h_1h_2+3h_2^2)+$$
$$k_{12}(h_1+h_2),$$

$$k_{32}=e^{2h_1k_0}(k_9(3h_1^2+3h_1h_2-2h_2^2)+k_{17}(h_1+h_2))-e^{2h_2k_0}(k_9(-2h_1^2+3h_1h_2+3h_2^2)+k_{17}(h_1+h_2)),$$

$$k_{33}=1296k_8(h_2^3(-8h_1^2+5h_1h_2+5h_2^2)e^{h_2k_0}-h_1^3(5h_1^2+5h_1h_2-8h_2^2)e^{h_1k_0}),$$

$$k_{34}=81k_9(h_2(-4h_1^2+3h_1h_2+3h_2^2)e^{2h_2k_0}-h_1(3h_1^2+3h_1h_2-4h_2^2)e^{2h_1k_0}),$$

$$k_{35}=-1296e^{h_1k_0}(2k_{12}(h_1^2+h_1h_2-h_2^2)+h_1(k_{13}(3h_1+3h_1h_2-4h_2^2)+2h_1k_{14}(2h_1^2+2h_1h_2-3h_2^2))+k_{11}(h_1+h_2))-16k_{10}(h_1+h_2)e^{3h_1k_0}+16k_{10}(h_1+h_2)e^{3h_2k_0}+k_{33}+k_{34},$$

$$k_{36}=1296e^{h_2k_0}(2k_{12}(-h_1^2+h_1h_2+h_2^2)+h_2(k_{13}(-4h_1^2+3h_1h_2+3h_2^2)+2h_2k_{14}(-3h_1^2+2hh_2+2h_2^2)+k_{11}(h_1+h_2)),$$

$$k_{37}=35k_0^4(-81e^{2h_1k_0}(2k_{17}(h_1^2+h_1h_2-h_2^2)+k_{15}(h_1+h_2))+81e^{2h_2k_0}(2k_{17}(-h_1^2+h_1h_2+h_2^2)+k_{15}(h_1+h_2))+k_{35}+k_{36}),$$

$$k_{38}=70k_0^5(h_1-h_2)(8k_{10}(2h_1+h_2)e^{3h_2k_0}+216(2h_1+h_2)e^{h_2k_0}(h_2(h_2(h_2(h_2k_8+k_{14})+k_{13})+k_{12})+k_{11})+27(2h_1+h_2)e^{2h_2k_0}(h_2(h_2k_9+k_{17})+k_{15})+(h_1+2h_2)e^{h_1k_0}(8k_{10}e^{2h_1k_0}+216(h_1(h_1(h_1(h_1k_8+k_{14})+k_{13})+k_{12})+k_{11})+27e^{h_1k_0}\left(h_1\left(h_1k_9+k_{17}\right)+k_{15}\right)),$$

$$k_{39}=5443200k_0(h_2e^{h_1k_0}\left(k_8\left(-10h_1^2+h_1h_2+h_2^2\right)-2h_1k_{14}\right)-h_1e^{h_2k_0}(k_8(h_1^2+h_1h_2-10h_2^2)-2h_2k_{14}))+76204800h_1h_2k_8\left(e^{h_1k_0}-e^{h_2k_0}\right),$$

$$k_{40}=28350k_0^2(h_2e^{h_1k_0}\left(64h_1\left(2k_8\left(5h_1^2-h_1h_2-h_2^2\right)+k_{13}\right)+32k_{14}\left(8h_1^2-h_1h_2-h_2^2\right)+h_1k_9e^{h_1k_0}\right)+32h_1e^{h_2k_0}\left(4h_2k_8\left(h_1^2+h_1h_2-5h_2^2\right)+k_{14}\left(h_1^2+h_1h_2-8h_2^2\right)-2h_2k_{13}\right)+h_1h_2k_9\left(-e^{2h_2k_0}\right)),$$

$$k_{41}=18h_1h_2k_0^8(h_1-h_2)^3(7k_{16}(4h_1^2+7h_1h_2+4h_2^2)+k_5(8h_1^4+17h_1^3h_2+20h_1^2h_2^2+17h_1h_2^3+8h_2^4)+(h_1+h_2)(14k_7(h_1^2+h_1h_2+h_2^2)+k_6(5h_1^4+6h_1^3h_2+8h_1^2h_2^2+6h_1h_2^3+5h_2^4))+70k_4(h_1+h_2)),$$

$$k_{42}=32h_2e^{h_1k_0}(2h_1^2k_8(-10h_1^2+3h_1h_2+3h_2^2)+3h_1k_{14}(-4h_1^2+h_1h_2+h_2^2)+k_{13}(-6h_1^2+h_1h_2+h_2^2)-2h_1k_{12}),$$

$$k_{43}=h_1e^{h_2k_0}(64h_2(h_2k_8(-3h_1^2-3h_1h_2+10h_2^2)+k_{12})-96h_2k_{14}(h_1^2+h_1h_2-4h_2^2)-32k_{13}(h_1-2h_2)(h_1+3h_2)+e^{h_2k_0}\left(2h_2k_{17}-k_9(h_1-2h_2)(h_1+3h_2)\right)),$$

$$k_{44}=5670k_0^3(h_2e^{2h_1k_0}(k_9(-6h_1^2+h_1h_2+h_2^2)-2h_1k_{17})+k_{42}+k_{43}),$$

$$k_{45}=1296h_1e^{h_2k_0}(h_2(2k_{13}(h_1^2+h_1h_2-3h_2^2)+h_2k_{14}(3h_1^2+3h_1h_2-8h_2^2)+k_{12}(h_1-4h_2)-2k_{11})+2h_2^3k_8(2h_1^2+2h_1h_2-5h_2^2)+h_1^2k_{12})-32h_1h_2k_{10}e^{3h_2k_0},$$

$$k_{46}=81h_1e^{2h_2k_0}\left(2h_2k_9\left(h_1^2+h_1h_2-3h_2^2\right)+k_{17}\left(h_1^2+h_1h_2-4h_2^2\right)-2h_2k_{15}\right)+k_{45},$$

$$k_{47}=-6h_1^3k_{13}+h_1^2k_{14}(-8h_1^2+3h_1h_2+3h_2^2)+2h_1^2h_2k_{13}-4h_1^2k_{12}+2h_1^3k_8(-5h_1^2+2h_1h_2+2h_2^2)+2h_1^2h_2k_{13}+h_1h_2k_{12}-2h_1k_{11}+h_2^2k_{12},$$

$$k_{48}=h_2e^{h_1k_0}(-81e^{h_1k_0}(2h_1k_9(-3h_1^2+h_1h_2+h_2^2)+k_{17}(-4h_1^2+h_1h_2+h_2^2)-2h_1k_{15})+32h_1k_{10}e^{2h_1k_0}-1296k_{47})+k_{46},$$

$$k_{49}=8h_1k_{10}(h_1+2h_2)e^{3h_2k_0}+$$
$$216h_1(h_1+2h_2)e^{h_2k_0}(h_2(h_2(h_2(h_2k_8+k_{14})+k_{13})$$
$$+k_{12})+k_{11})+27h_1(h_1+2h_2)e^{2h_2k_0}(h_2(h_2k_9+k_{17})+k_{15}),$$

$$k_{50}=70k_0^5(h_1-h_2)(h_2(2h_1+h_2)e^{h_1k_0}(8k_{10}e^{2h_1k_0}+$$
$$216(h_1(h_1(h_1(h_1k_8+k_{14})+k_{13})+k_{12})+k_{11})+$$
$$27e^{h_1k_0}(h_1(h_1k_9+k_{17})+k_{15}))+k_{49}),$$
$$k_{51}=38102400k_8(h_1^2(3h_2-h_1)e^{h_2k_0}+$$
$$h_2^2(h_2-3h_1)e^{h_1k_0}),$$

$$k_{52}=5443200k_0(h_1^2e^{h_2k_0}(h_2k_8(7h_1-15h_2)+$$
$$k_{14}(h_1-3h_2))+h_2^2e^{h_1k_0}(h_1k_8(15h_1-7h_2)+k_{14}(3h_1-h_2))),$$

$$k_{53}=64h_2^2e^{h_1k_0}(6h_1^2k_8(3h_2-5h_1)+6h_1k_{14}(h_2-2h_1)+$$
$$k_{13}(h_2-3h_1))+h_2^2k_9(h_2-3h_1)e^{2h_1k_0},$$

$$k_{54}=14175k_0^2(h_1^2e^{h_2k_0}(64(6h_2^2k_8(5h_2-3h_1)-$$
$$6h_2k_{14}(h_1-2h_2)-k_{13}(h_1-3h_2))+k_9(3h_2-h_1)e^{h_2k_0})+k_{53}),$$

$$k_{55}=12k_5(h_1+h_2)(2h_1^2+h_1h_2+2h_2^2)+$$
$$14k_7(3h_1^2+4h_1h_2+3h_2^2)+3k_6(5h_1^4+8h_1^3h_2+9h_1^2h_2^2+$$
$$8h_1^3h_2+5h_2^4)+84k_{16}(h_1+h_2)+210k_4,$$

$$k_{56}=9k_0^8(h_1^2h_2^2k_{55}(h_1-h_2)^3),$$

$$k_{57}=32h_1^2e^{h_2k_0}(2h_2^3k_8(11h_1-15h_2)+$$
$$h_2(k_{13}(5h_1-9h_2)+6h_2k_{14}(2h_1-3h_2))+k_{12}(h_1-3h_2)),$$

$$k_{58}=5670k_0^3(h_2^2e^{h_1k_0}(32(2h_1^3k_8(15h_1-11h_2)+$$
$$h_1(k_{13}(9h_1-5h_2)+6h_1k_{14}(3h_1-2h_2))+k_{12}(3h_1-h_2))+,$$
$$e^{h_1k_0}(h_1k_9(9h_1-5h_2)+k_{17}(3h_1-h_2)))+$$
$$h_1^2e^{2h_2k_0}(h_2k_9(5h_1-9h_2)+k_{17}(h_1-3h_2))+k_{57}),$$

$$k_{59}=1296h_1^2h_2^2k_8(h_2^2(15h_2-13h_1)e^{h_2k_0}-$$
$$h_1^2(15h_1-13h_2)e^{h_1k_0})+16h_2^2k_{10}(h_2-3h_1)e^{3h_1k_0}$$

$$k_{60}=1296h_2^2e^{h_1k_0}(k_{11}(h_2-3h_1)+$$
$$h_1(k_{12}(4h_2-6h_1)+h_1(k_{13}(7h_2-9h_1)+$$
$$2h_1k_{14}(5h_2-6h_1)))),$$
$$k_{61}=81h_2^2e^{2h_1k_0}(h_1^2k_9(7h_2-9h_1)+2h_1k_{17}(2h_2-3h_1)+$$
$$k_{15}(h_2-3h_1)),$$

$$k_{62}=h_1^2e^{h_2k_0}(81e^{h_2k_0}(h_2^2k_9(9h_2-7h_1)+$$
$$2h_2k_{17}(3h_2-2h_1)-k_{15}(h_1-3h_2))+$$
$$16k_{10}(3h_2-h_1)e^{2h_2k_0}-1296(k_{11}(h_1-3h_2)+$$
$$h_2(k_{12}(4h_1-6h_2)+h_2(k_{13}(7h_1-9h_2)+$$
$$2h_2k_{14}(5h_1-6h_2))))),$$

$$k_{63}=210h_1h_2k_0^5(h_1-h_2h_1)(8k_{10}e^{3h_2k_0}+$$
$$216h_1e^{h_2k_0}(h_2(h_2(h_2(h_2k_8+k_{14})+k_{13})+k_{12})+k_{11})+$$
$$27h_1e^{2h_2k_0}(h_2(h_2k_9+k_{17})+k_{15})+$$
$$h_2e^{h_1k_0}(8k_{10}e^{2h_1k_0}+216(h_1(h_1(h_1(h_1k_8+k_{14})+k_{13})+$$
$$k_{12})+k_{11})+27e^{h_1k_0}(h_1\left(h_1k_9+k_{17}\right)+k_{15}))),$$

$$b_{00}=k_{18}+k_{19}-k_{20}+k_{21}+k_{23}+k_{24},$$

$$b_{01}=5670k_0^3(-32k_{31}e^{h_2k_0}+k_{30}+k_{32})+$$
$$9\left(k_{28}+k_{29}\right)k_0^8+k_{25}+k_{26}+k_{27}+k_{37}+k_{38},$$

$$b_{02}=35k_{48}k_0^4+k_{39}+k_{40}-k_{41}+k_{44}-k_{50},$$

$$b_{03}=35\left(k_{59}+k_{60}+k_{61}+k_{62}\right)k_0^4+k_{51}+$$
$$k_{52}+k_{54}+k_{56}+k_{58}+k_{63},$$

$$b_{04}=\frac{1}{24\left(h_1-h_2\right)^3k_0^4}\left(h_1(-Brh_2^4k_2k_0^4-24h_2k_3k_0e^{h_2k_0}+\right.$$
$$72k_3e^{h_2k_0}+24k_3e^{h_1k_0}\left(h_2k_0-3\right)+72k_0^4q)+$$
$$h_2(-Brh_2^4k_2k_0^4+72(k_3\left(e^{h_2k_0}-e^{h_1k_0}\right)+$$
$$k_0^4q)-24h_2k_0\left(k_3\left(2e^{h_1k_0}+e^{h_2k_0}\right)+3k_0^3\right))+$$
$$Brh_1^5k_0^4k_2+Brh_2h_1^4k_0^4k_2-8Brh_2^2h_1^3k_0^4k_2+$$
$$\left.8h_1^2k_0(k_0^3(Brh_2^3k_2+9)+3k_3\left(e^{h_1k_0}+2e^{h_2k_0}\right))\right),$$

$$b_{05}=\frac{1}{12\left(h_1-h_2\right)^3k_0^4}\left(24k_3\left(e^{h_1k_0}-e^{h_2k_0}\right)+\right.$$
$$k_0\left(-Brh_1^4k_0^3k_2+2Brh_2h_1^3k_0^3k_2-\right.$$
$$2h_1\left(k_0^3\left(Brh_2^3k_2+12\right)+6k_3\left(e^{h_1k_0}+e^{h_2k_0}\right)\right)+$$
$$\left.\left.Brh_2^4k_0^3k_2-24k_0^3q+2k_0^3+12h_2\left(k_3\left(e^{h_1k_0}+e^{h_2k_0}\right)\right)\right)\right),$$

Received : Dec. 8, 2014 ; Accepted : Aug. 1, 2016

REFERENCES

[1] Choi, Enhancing Thermal Conductivity of Fluid with Nanoparticles Developments and Applications of Non-Newtonian Flow, *ASME FED*, **66**: 99-105 (231).

[2] Selvakumar P., Suresh S., Convective Performance of CuO/Water Nanofluid in an Electronic Heat Sink, *Experimental Thermal and Fluid Science*, **40**: 57-63 (2012).

[3] Bachok N., Ishak A., Pop I., Boundary-Layer Flow of Nanofluids Over a Moving Surface in a Flowing Fluid, *International Journal of Thermal Sciences*, **49**: 1663-1668 (2010).

[4] Aziz A., Khan W.A., Natural Convective Boundary Layer Flow of a Nanofluid Past a Convectively Heated Vertical Plate, *International Journal of Thermal Sciences*, **52**: 83-90 (2012).

[5] Aziz A., Khan W.A., Pop I., Free Convection Boundary Layer Flow Past a Horizontal Flat Plate Embedded in Porous Medium Filled by Nanofluid Containing Gyrotactic Microorganisms, *International Journal of Thermal Sciences*, **56**: 48-57 (2912).

[6] Rahman S.U., Ellahi R., Nadeem S., Zaigham Zia Q.M., Simultaneous Effects of Nanoparticles and Slip on Jeffrey Fluid Through Tapered Artery with Mild Stenosis, *Journal of Molecular Liquids*, **218**: 484-493 (2016).

[7] Sheikholeslami M., Ellahi R., Electrohydrodynamic Nanofluid Hydrothermal Treatment in an Enclosure with Sinusoidal Upper Wall, *Applied Sciences*, **5**: 294-306 (2015).

[8] Noreen Sher Akbar, Raza M., Ellahi R., Influence of Induced Magnetic Field and Heat Flux with the Suspension of Carbon Nanotubes for the Peristaltic Flow in a Permeable Channel, *Journal of Magnetism and Magnetic Materials*, **381**: 405-415 (2015).

[9] Ellahi R., Hassan M., Zeeshan A., Study of Natural Convection MHD Nanofluid by Means of Single and Multi-Walled Carbon Nanotubes Suspended in a Salt-Water Solution, *IEEE Transactions on Nanotechnology*, **14**: 726-734 (2015).

[10] Sheikholeslami M., Ellahi R., Three Dimensional Mesoscopic Simulation of Magnetic Field Effect on Natural Convection of Nanofluid, *International Journal of Heat and Mass Transfer*, **89**: 799-808 (2015).

[11] Ellahi R., Hassan M., Zeeshan A., Shape Effects of Nanosize Particles in Cu-H_2O Nanofluid on Entropy Generation, *International Journal of Heat and Mass Transfer*, **81**: 449-456 (2015).

[12] Sheikholeslami M., Ganjia D.D., Younus Javed M., Ellahi R., Effect of Thermal Radiation on Magnetohydrodynamics Nanofluid Flow and Heat Transfer by Means of Two Phase Model, *Journal of Magnetism and Magnetic Materials*, **374**: 36-43 (2015).

[13] Latham T.W., "Fluid Motion in a Peristaltic Pump", MSc. Thesis, MIT, Cambridge, MA. (1966) .

[14] Eytan O., Jaffa A.J., Elad D., Peristaltic Flow in a Tapered Channel: Application to Embryo Transport Within the Uterine Cavity, *Medical Engineering and Physics*, **23**: 475-484 (2001).

[15] Tripathi D., Peristaltic Transport of a Viscoelastic Fluid in a Channel, *Acta Astronautica*, **68**: 1379-1385 (2011).

[16] Kothandapani M., Srinivas S., Non-Linear Peristaltic Transport of a Newtonian Fluid in an Inclined Asymmetric Channel Through a Porous Medium, *Physics Letters A*, **372**: 1265-1276 (2008).

[17] Srinivas S., Gayathri R., Kothandapani M., Mixed Convective Heat and Mass Transfer in an Asymmetric Channel with Peristalsis, *Communications in Nonlinear Science and Numerical Simulation*, **16**: 1845-1862 (2011).

[18] Yldrm A., Sefa Anl Sezer, Effects of Partial Slip on the Peristaltic Plow of a MHD Newtonian Fluid in an Asymmetric Channel, *Mathematical and Computer Modeling*, **52**: 618-625 (2010).

[19] Nadeem S., Akbar N.S., Influence of Heat and Mass Transfer on a Peristaltic Motion of a Jeffrey-Six Constant Fluid in an Annulus, *Heat and Mass Transfer*, **46**: 485-493 (2010).

[20] Haroun M.H., Non-Linear Peristaltic Flow of a Fourth Grade Fluid in an Inclined Asymmetric Channel, *Computer Material Science*, **39**: 324-333 (2007).

[21] Haroun M.H., Effect of Deborah Number and Phase Difference on Peristaltic Transport of a Third Order Fluid in an Asymmetric Channel, *Communications in Nonlinear Science and Numerical Simulation*, **12**: 1464-1480 (2007).

[22] Zeeshan A., Majeed A., Ellahi R., Effect of Magnetic Dipole on Viscous Ferro-Fluid Past a Stretching Surface with Thermal Radiation, *Journal of Molecular Liquids*, **215**: 549-554 (2016).

[23] Rashidi S., Dehghan M., Ellahi R., Riaz M., Jamal-Abad M.T., Study of Stream Wise Transverse Magnetic Fluid Flow with Heat Transfer Around an Obstacle Embedded in a Porous Medium, *Journal of Magnetism and Magnetic Materials*, **378**: 128-137.

[24] Sheikholeslami M., Ellahi R., Simulation of Ferrofluid Flow for Magnetic Drug Targeting Using the Lattice Boltzmann Method, *Zeitschrift für Naturforschung A*, **70**: 115-124 (2015).

[25] Boger D.V., Demonstration of Upper and Lower Newtonian Fluid Behavior in a Pseudoplastic Fluid, *Nature*, **265**: 126-128 (1977).

[26] Nadeem S., Akram S., Slip Effects on the Peristaltic Flow of a Jeffrey Fluid in an Asymmetric Channel Under the Effect of Induced Magnetic Field, *International Journal for Numerical Methods in Fluids*, **63**: 374-394 (2010).